

## Research Article

# The Schizophrenia Variant V1282F in *SCN2A* Causes Functional Impairment of Na<sub>v</sub>1.2

Kohlhofer B, Liu Y, Woodruff G, Lovenberg T, Bonaventure P and Harrington AW\*

Neuroscience Discovery, Janssen Pharmaceutical Companies of Johnson & Johnson, USA

\*Corresponding author: Anthony W Harrington, Neuroscience Discovery, Janssen Pharmaceutical Companies of Johnson & Johnson, 3210 Merryfield Row, San Diego, CA 92121, USA

Received: March 17, 2021; Accepted: April 01, 2021;

Published: April 08, 2021

## Abstract

Neuropsychiatric disorders such as schizophrenia are challenging to treat due to the biological complexity of the disease and the lack of knowledge of the underlying pathophysiology. Whole exome and genome sequencing studies have identified disease-linked rare variants in patients with large effect size. Here, we functionally characterize the schizophrenia linked variant V1282F in *SCN2A*, encoding the sodium channel Na<sub>v</sub>1.2. This variant was introduced into isogenic lines of hiPSCs using CRISPR/CAS9 genome editing tools. hiPSCs were then differentiated into cortical neurons to understand how the variant and gene may be contributing to disease. We observed a significant (~25%) decrease in sodium current in the V1282F neurons compared to control neurons, suggesting the mutation is causing a loss-of-channel function. These results were supported by recordings in recombinant cells overexpressing either the mutant or wildtype Na<sub>v</sub>1.2, with the mutant channel having significantly (~75%) lower current amplitude than wildtype. We hypothesize that this phenotype may contribute to disease either through the direct loss of neuronal activity or through subsequent abnormal neurodevelopment.

## Introduction

Elucidating novel therapeutic targets for schizophrenia has been difficult due to the lack of knowledge of the fundamental biology and pathophysiology of this complex disease. Additionally, there is poor predictive validity in current pre-clinical models. Factoring into these problems is the lack of human model systems and our poor understanding of the disease genetics. Genetics are a major contributor to schizophrenia, as the heritability of schizophrenia is estimated to be 79% from twin studies [1]. With the recent advances in genome sequencing, we now have insight into genes that may be contributing to schizophrenia and that have the potential to be novel pharmaceutical targets. Genome Wide Association Studies (GWAS) and whole genome or exome sequencing efforts have identified variants in schizophrenia patients, presumed to be disease causing but it is not clear what the functional effects of these variants are, if any. Most of the GWAS-identified common variants are within non-coding regions, so the field resorts to investigating rare coding variants identified through whole genome or exome sequencing. To transition from the bench to the bedside, it is necessary to first understand how individual patient risk variants affect gene or gene product function and how this contributes to disease.

Many of the genes that contain variants for schizophrenia overlap with those that contain variants for Autism Spectrum Disorder (ASD) and Intellectual Disability (ID) [2]. The gene that harbors the greatest combined number of variants identified in ASD, ID, and schizophrenia patient populations is the voltage-gated Sodium Channel Alpha Subunit 2 (*SCN2A*). *SCN2A* encodes for the sodium channel Na<sub>v</sub>1.2, which is critical for the initiation and propagation of action potentials [3]. In fact, in excess of a hundred unique *de novo* mutations in *SCN2A* have been identified and with hundreds of children born each year having mutations in *SCN2A* [4,5]. These

variants have been identified through whole genome or exome sequencing studies and although extremely rare, they are expected to have high penetrance. *SCN2A* variants have also been identified in patients with Infantile Epileptic Encephalopathy (IEE) and Benign Infantile Familial Seizures (BIFS), where the contribution of variants to disease is better understood and those variants that have been functionally analyzed have been found to be gain-of-function [6-11]. Through bioinformatic modeling, multiple *SCN2A* variants identified in neuropsychiatric patients were predicted to be loss-of-function and recently a few have been functionally evaluated using overexpression studies in HEK293 cells. Eleven unique ASD variants and three unique ID variants were found to either functionally inactive or inhibit channel function [12,13]. In mice, *SCN2A* knockout is embryonic lethal and multiple groups have found that *SCN2A*<sup>-/-</sup> mice display autistic and schizophrenia-like phenotypes [14-16].

While schizophrenia-linked mutations in *SCN2A* are less common, mutations have been identified through whole genome or exome sequencing, including one that leads to loss of a splice site (c.2150 A>G), one that generates a nonsense mutation (E169X), and one that creates a missense mutation (V1282F) [2,17]. However, none of them have been functionally investigated [2,17-19]. To date, there are no reports on the functionality or effect of *SCN2A* variants associated with schizophrenia. In this study, we investigated one coding variant, V1282F (Chr2: 166226804, (G/T)), located in the third transmembrane segment of the third domain. This is a missense variant that has been identified in two unrelated patients and is absent in the control dataset [17]. To investigate this variant in a biologically relevant system, we used human induced pluripotent stem cell (hiPSC) derived cortical neurons and introduced the variant using CRISPR/CAS9 genome editing tools to analyze the variant under endogenous expression levels. We found that the V1282F variant causes a significant decrease in Na<sup>+</sup> channel current density. V1282F

mutant channels exogenously expressed in HEK293 cells further showed lower current amplitudes than Wildtype (WT) channels, consistent with the findings in hiPSC-derived neurons and suggesting a loss-of-channel function associated with the V1282F mutant. To our knowledge, this is the first report of the functional impact of a *SCN2A* variant identified in a schizophrenia patient.

## Methods

### hiPSC maintenance and genome editing

The healthy control hiPSC line GM25430 (CVB) was obtained from the Coriell Institute (Camden, NJ). All hiPSC lines were maintained in mTeSR on vitronectin coated plates passaged using ReLeSR (Stem Cell Technologies, Vancouver, Canada). To generate *SCN2A*<sup>WT/V1282F</sup> and *SCN2A*<sup>V1282F/V1282F</sup> hiPSC lines, a guide RNA (gcatactcacATCAACAATC) was designed to target exon 19 near chromosome position: 166226804(G/T) using the guide design tool from crispr.mit.edu and a SSODN donor template was designed using 50bp homology arms incorporating the (G/T) variant (G T T T T C A A G T G T A T T T T A C C A A T G C C T G G T G C T G G C T A G A C T T C C T G A T T (T) T T G A T G T G A G T A T G C T G C A C T T T G C T G C T T T A T T C A T T G G C A T A T A T G T). Genome editing was performed using the Alt-R-CRISPR system (IDT, Coralville, IA). Alt-R S.p. HiFi Cas9 Nuclease V3, Alt-R CRISPR-Cas9 crRNA, Alt-R CRISPR-Cas9 tracrRNA (ATTO 550), and SSODN were nucleofected into hiPSCs using the P3 Primary Cell 4D-Nucleofector X kit and the Amaxa 4D-Nucleofector X Unit (Lonza, Basel, Switzerland) setting CB-150. 24 hours post-nucleofection ATTO 550+ single cells were FACS sorted and plated. Isogenic clones were screened for the variant by amplifying the DNA using Polymerase Chain Reaction (PCR) and primers flanking the variant (Primer F: aggagttctgcaaatgagttacc and Primer R: aatgtttgaggcatcctctcactg) followed by Sanger sequencing.

### Neural precursor cell differentiation and neuron differentiation

hiPSCs were differentiated into Neural Precursor Cells (NPCs) over the course of three weeks using the STEMdiff Neural Induction Media + SMADi Kit and protocol (STEMCELL Technologies) on 0.01% Poly-L-ornithine and Laminin (ThermoFisher, Waltham, MA) coated plates. NPCs were cultured in neural maintenance media: 0.5X DMEM/F12 + Glutamax, Neurobasal, 0.5X N2 supplement, 0.5X B27 Supplement, 0.5X Glutamax, 0.5X IT-S, 0.25X 2-Mercaptoethanol (Gibco-ThermoFisher, Waltham, MA), Pen-Strep (Corning, Corning, NY) and NEAA (Hyclone Laboratories Inc- ThermoFisher, Waltham, MA), and 20ng/ml FGF2 (R&D Systems, Minneapolis, MN). NPCs were differentiated into neurons by withdrawing FGF2 once confluent. After three weeks, cells were replated for downstream assays and 24 hours later treated with 1uM cytosine arabinoside (ARA-C) (Sigma, St. Louis, MO) for 72 hours to eliminate proliferating cells. After ARA-C treatment the media was switched to neuronal maturation media containing Brain Phys (STEMCELL Technologies), 1X PenStrep, 1X N2 supplement, 1X B27 Supplement, 20ng/uL BDNF (Peprotech, Rocky Hill, NJ), 20ng/uL GDNF (Peprotech), 1mM cAMP (Sigma, St. Louis, MO), 1ug/mL Laminin, and 200nM Ascorbic Acid (Sigma). Neurons were matured for an additional month with weekly half media changes. All assays were performed at eight weeks after FGF2 withdrawal unless

indicated.

### RNA isolation, cDNA synthesis and qRT-PCR

RNA was isolated from hiPSCs or two-month neuronal cultures using a RNeasy Mini Kit and samples were DNase treated on column (Qiagen, Hilden, Germany). cDNA was synthesized using SuperScript IV First-Strand Synthesis System (Invitrogen, Carlsbad, CA) and qRT-PCR was performed using TaqMan assays (ThermoFisher, Waltham, MA) and analyzed on a QuantStudio Real Time PCR System (Applied Biosystems, Foster City, CA). TaqMan assays: OCT4: Hs00999634\_gH, *SCN2A*: Hs01109871\_m1, *SCN3A*: Hs00366902\_m1, *SCN8A*: Hs00274075\_m1, and *GAPDH*: Hs02786624\_g1. Data were normalized to *GAPDH* expression levels. Data were plotted as mean  $\pm$ SEM. Statistical analysis was performed using a one-way ANOVA and results were considered significant at p-value <0.05 (GraphPad Prism).

### Immunofluorescence

NPCs were fixed in 4% Paraformaldehyde (PFA) for five minutes and two-month neuronal cultures were fixed in with 4% PFA for 30 minutes. Samples were permeabilized and blocked in 0.5% PB-Triton and 5% BSA for one hour. Primary antibodies: anti-Na<sub>v</sub>1.2, Cat#: ASC-002 (Alomone Labs, Jerusalem, Israel); MAP2, Cat#: AB5392 (Abcam, Cambridge, United Kingdom); SYP, Cat#: AB14692 (Abcam); SOX2, Cat#: AB97959 (Abcam); NES, Cat#: ab22035 (Abcam) were incubated at 4°C overnight and secondary antibodies were incubated at room temperature for one hour. Images were captured on an Opera Phenix high-content imager at 20x magnification (PerkinElmer, Waltham, MA) and analyzed using their Columbus Image Data Storage and Analysis System software. Synapse density was quantified by having the software find puncta in the area surrounding the neurites. Images were analyzed from two lines from each genotype, three differentiations, with at least six wells with five images from each well. Data were plotted as mean  $\pm$ SEM. Statistical analysis was performed using a one-way ANOVA and results were considered significant at p-value <0.05 (GraphPad Prism).

### *SCN2A* pulldown and simple western blot- protein simple wes/jess platform

Na<sub>v</sub>1.2 membrane protein was isolated from two-month neurons by preincubation of the neurons with the 100ug/ml leupeptin (Sigma) for 30 minutes at 37°C, biotinylation of membrane proteins in 1.5mg/ml sulfo-NHS-SS-biotin (Sigma) for 20 minutes at 4°C rotating, cell lysis, and pull-down of the biotinylated protein using neutravidin-agarose beads (Pierce, Waltham, MA). Both membrane Na<sub>v</sub>1.2 and total Na<sub>v</sub>1.2 samples were probed using Na<sub>v</sub>1.2 ASC-002 (Alomone Labs) at 1:500 *via* western using the Jess High Molecular Weight 66-440 kDa Separation Module (Protein Simple, San Jose, CA). Total Na<sub>v</sub>1.2 samples were normalized to total protein using the Protein Simple- Total Protein Assay (Protein Simple) and membrane Na<sub>v</sub>1.2 was normalized to input Na<sub>v</sub>1.2 protein. Data were plotted as mean  $\pm$ SEM. Statistical analysis was performed using a one-way ANOVA and results were considered significant at p-value <0.05 (GraphPad Prism).

### Electrophysiology

For manual patch clamp recording, neurons were cultured at a density of  $3 \times 10^5$  cells on 15mm glass coverslips placed in a chamber on

the stage of an inverted microscope. Upon formation of the whole-cell conformation, the cell was constantly perfused with an extracellular solution containing (in mM): 74.5 NaCl, 74.5 choline Cl, 2.5 BaCl<sub>2</sub>, 2 KCl, 1 MgCl<sub>2</sub>, 5 glucose, 10 HEPES, 0.3 CdCl<sub>2</sub>, 3 4-aminopyridine, pH 7.4, 310 mOsm/L. The pipette electrode was filled with an intracellular solution containing (in mM): 115 Cs methanesulfonate, 20 CsCl, 3 NaCl, 4 MgATP, 0.3 Na<sub>2</sub>GTP, 10 EGTA and 20 HEPES, pH 7.2, 290 mOsm/L. Currents were measured by whole-cell patch clamp using an Axopatch 200B amplifier and pClamp 11 software (Molecular Devices, San Jose, CA), digitized at 20 kHz and lowpass filtered at 5 kHz. Series resistance was 75% compensated. Currents were leak subtracted using a P/4 protocol.

For automated SyncroPatch electrophysiology (Nanion, Germany), cDNA of the  $\alpha$  subunit of the human Na<sub>v</sub>1.2 WT and V1282F mutant was transfected into HEK293 cells (76  $\mu$ g each per T75 flask). Transfected cells were kept at 37°C for the first day and moved to 30°C for the second day before experiment. Single-hole chips with medium resistance were used. The extracellular solution contained (in mM): 149 NaCl, 2.8 CaCl<sub>2</sub>, 4 KCl, 1 MgCl<sub>2</sub>, 5 glucose, 10 HEPES, pH 7.4, 310 mOsm/L. The intracellular solution contained (in mM): 110 CsF, 10 NaCl, 10 KCl, 10 EGTA, 10 HEPES, pH 7.2, 280 mOsm/L. Currents were digitized at 20 kHz and lowpass filtered at 5 kHz. Series resistance was automatically compensated. Currents were leak subtracted.

The voltage protocol was the same for both manual and automated patch clamp. From a holding potential of -100 mV, a 100-ms preconditioning pulse ranging from -100 mV to +40 mV (in 10 mV increments) was followed by a 10 ms test pulse to 0 mV and subsequent return to -100 mV. The time interval between preconditioning pulses was five seconds. The peak current amplitudes during the preconditioning pulses were used to calculate the voltage dependence of activation (I-V/G-V). The peak current amplitudes during the test pulses were used to calculate the current density and voltage dependence of inactivation. All electrophysiological recordings were performed at room temperature.

### Electrophysiology data analysis

$V_{1/2}$ , the voltage at which the conductance is 50% of the maximum value, was obtained by fitting the conductance-voltage (G-V) relationship to a Boltzmann function. Kinetic parameters were obtained by fitting the data with a single exponential function. Data fitting and statistical analyses (two-tailed Student's t-test or two-way ANOVA as indicated) were performed using Origin (Northampton, MA, USA). Results were considered statistically significant at p-value <0.05. Experimental data are reported as mean  $\pm$ SEM, which result from independent measurements on n different cells.

## Results

### Generation and characterization of isogenic SCN2A V1282F hiPSCs and neurons

To investigate whether the *SCN2A*<sup>V1282F/V1282F</sup> variant has any effect in hiPSC-derived cortical neurons, we used CRISPR/CAS9 genome editing tools to introduce the (G/T) variant into control hiPSCs. The (G/T) variant is in exon 19 and results in the substitution of a valine residue for a phenylalanine residue in the third segment of the third transmembrane domain in Na<sub>v</sub>1.2 (Figure 1A). This variant has been

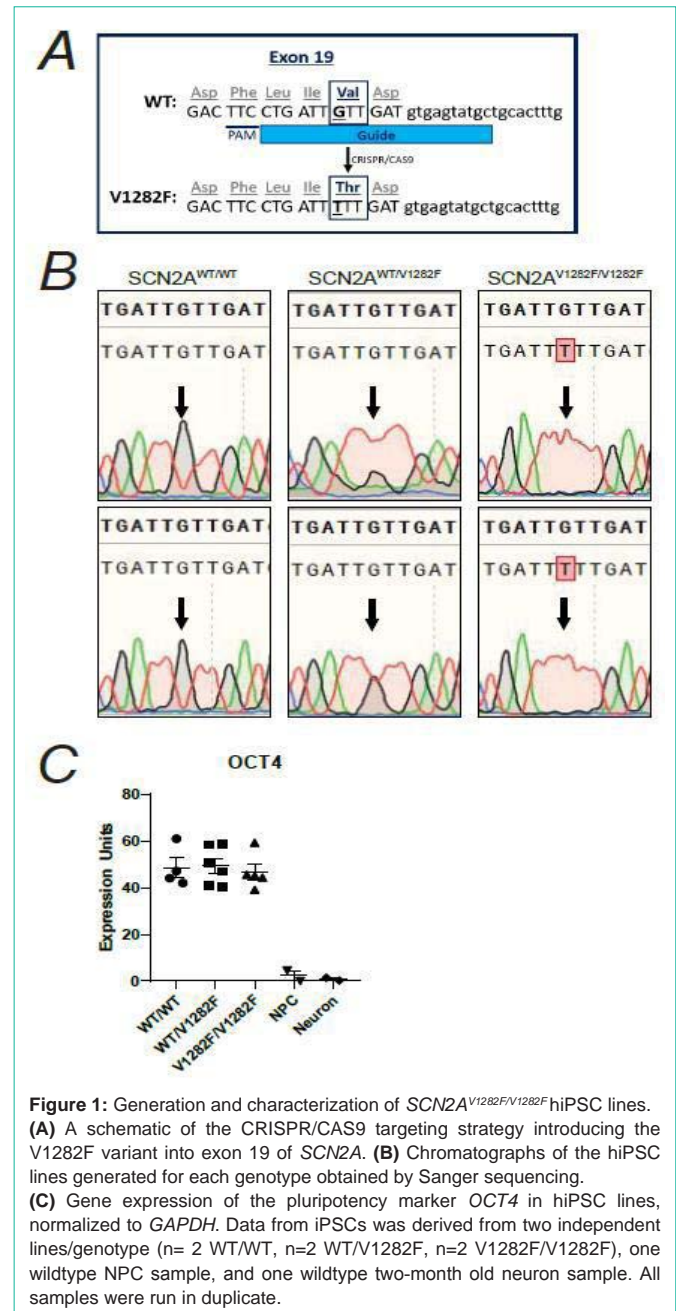
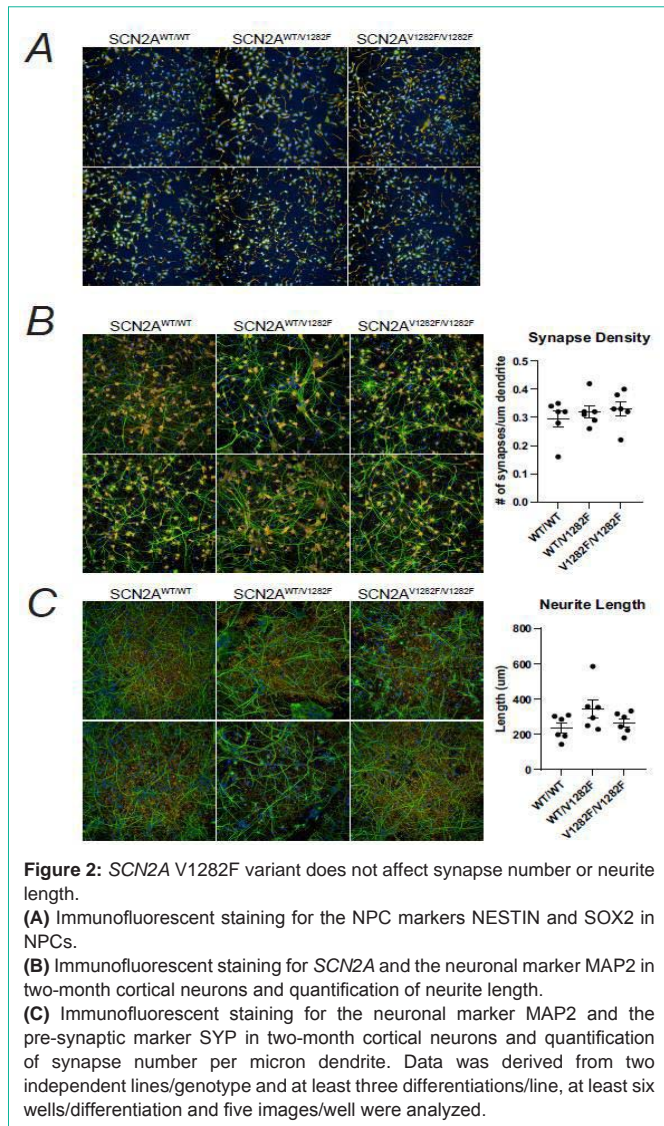


**Figure 1:** Generation and characterization of *SCN2A*<sup>V1282F/V1282F</sup> hiPSC lines. (A) A schematic of the CRISPR/CAS9 targeting strategy introducing the V1282F variant into exon 19 of *SCN2A*. (B) Chromatographs of the hiPSC lines generated for each genotype obtained by Sanger sequencing. (C) Gene expression of the pluripotency marker *OCT4* in hiPSC lines, normalized to *GAPDH*. Data from iPSCs was derived from two independent lines/genotype (n= 2 WT/WT, n=2 WT/V1282F, n=2 V1282F/V1282F), one wildtype NPC sample, and one wildtype two-month old neuron sample. All samples were run in duplicate.

identified in two schizophrenia patients, is absent from the control EVS population and statistics suggest this is a nonrandom association by the Fischer's exact test, 2-tailed p-value=0.034 [17]. However, the functional effects of V1282F are unknown.

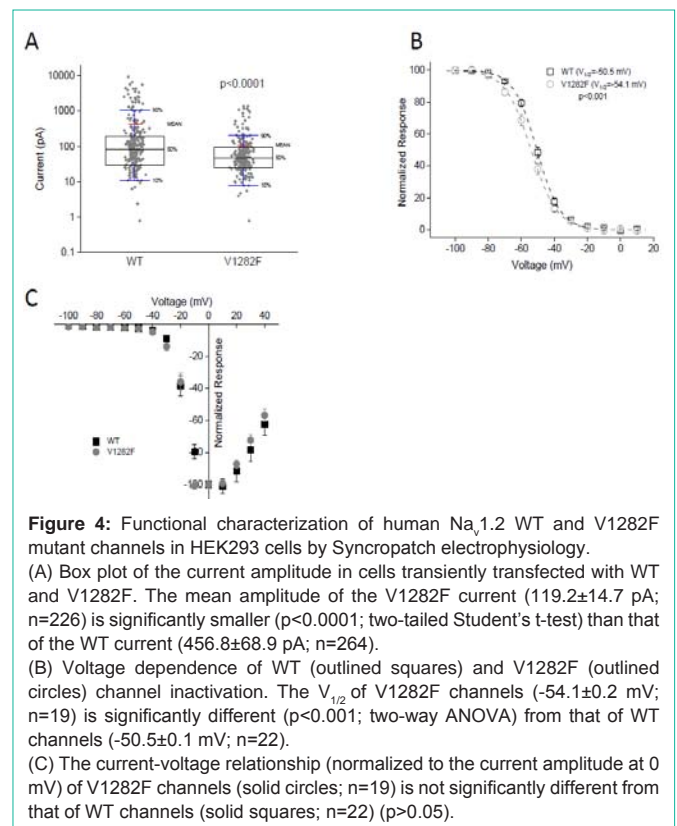
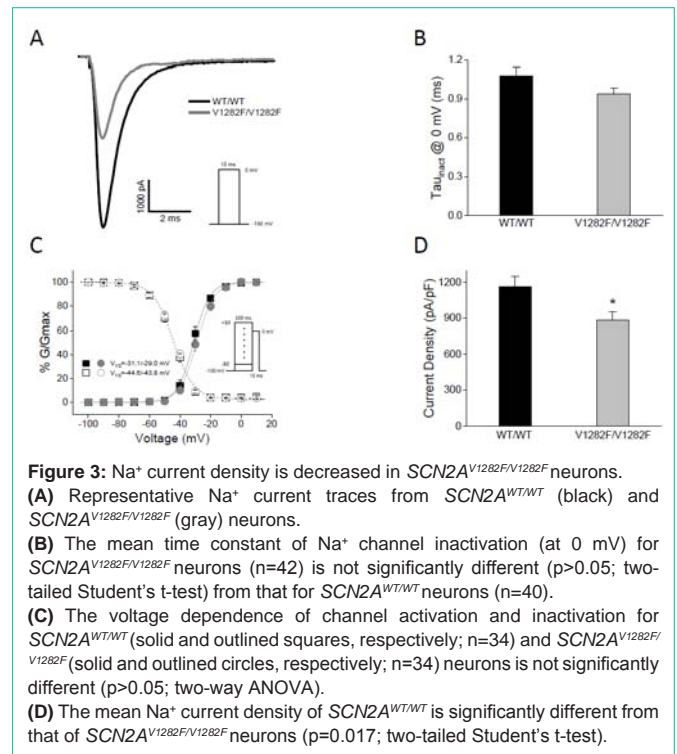
We generated two hiPSC lines for each genotype: wildtype homozygous (G/G) *SCN2A*<sup>WT/WT</sup>, heterozygous (G/T) *SCN2A*<sup>WT/V1282F</sup>, and V1282F homozygous (T/T) *SCN2A*<sup>V1282F/V1282F</sup> (Figure 2B). The hiPSC lines were confirmed to express the pluripotent stem cell transcript *OCT4* (Figure 1C), which confirms that the genome editing process did not affect pluripotency of the resulting isogenic clones. All hiPSCs were differentiated into Neural Precursor Cells (NPCs) and probed for the NPC proteins SRY-box transcription factor 2 (SOX2) and Nestin to confirm NPC identity (Figure 2A). NPCs were



differentiated down the cortical neuronal lineage and cultured for two months. We first characterized the control and variant neurons by staining for the Microtubule Associated Protein 2 (MAP2) and the presynaptic protein Synaptophysin (SYP) and analyzed neurite length and synapse density. We observed no significant differences in neurite length or synapse density between the three genotypes (Figure 2B and 2C). Together these data suggest that the variant does not affect neuronal differentiation, neurite elongation or synapse formation at this early stage *in vitro*.

**Sodium current density in SCN2A<sup>V1282F/V1282F</sup> neurons is decreased**

To determine if the missense variant alters Na<sup>+</sup> channel properties in these neurons, we performed whole-cell manual patch clamp studies on SCN2A<sup>WT/WT</sup> and SCN2A<sup>V1282F/V1282F</sup> neurons. No significant differences ( $p > 0.05$ ) in the kinetics of channel inactivation (Figure 3A and 3B) or the voltage dependence of channel activation and inactivation (Figure 3C) were observed between SCN2A<sup>WT/WT</sup> and SCN2A<sup>V1282F/V1282F</sup> neurons. However, the mean Na<sup>+</sup> current density in SCN2A<sup>V1282F/V1282F</sup> neurons ( $881.5 \pm 73.8$ ,  $n=45$ ) was



significantly ( $p=0.017$ ) smaller (by ~25%) than that in SCN2A<sup>WT/WT</sup> neurons ( $1162.7 \pm 88.5$ ,  $n=42$ ) (Figure 3A and 3D), suggesting that the SCN2A<sup>V1282F/V1282F</sup> variant may alter Na<sub>v</sub>1.2 channel function (e.g. channel open probability, single channel conductance, etc.) or the

number of functional Na<sub>v</sub>1.2 and/or other Na<sup>+</sup> channels at the cell surface.

### V1282F mutant channels have decreased whole-cell current amplitude in HEK293 cells

Since this is a native model system in which other sodium channels are likely contributing to the overall sodium current, we cannot isolate the sole contribution of Na<sub>v</sub>1.2 from the overall current. To better understand the functional effect of the variant on Na<sub>v</sub>1.2 channel specifically, we recorded from HEK293 cells transiently transfected with either Na<sub>v</sub>1.2 WT or V1282F mutant channels using the SyncroPatch automated patch clamp instrument. The V1282F channel was functional but when compared to the WT channel, the mean amplitude of the whole-cell current in cells expressing V1282F mutant channels was significantly smaller (by ~75%;  $p < 0.0001$ ) (Figure 4A). In addition, V1282F produced a relatively small (~3.5 mV), but statistically significant ( $p < 0.001$ ), hyperpolarizing shift in the voltage dependence of channel inactivation (Figure 4B). The voltage dependence of channel activation, on the other hand, was not significantly ( $p > 0.05$ ) different between WT and V1282F channels (Figure 4C).

### SCN2A V1282F variant does not alter Na<sub>v</sub>1.2 membrane expression or localization

A decrease in sodium current could be caused by a decrease in SCN2A expression level or a decrease in the number of Na<sub>v</sub>1.2 channels present at the plasma membrane. To investigate these theories, we measured SCN2A gene expression, protein and membrane localization levels in SCN2A<sup>WT/WT</sup>, SCN2A<sup>WT/V1282F</sup>, and SCN2A<sup>V1282F/V1282F</sup> neurons. We found that SCN2A gene expression was unaltered between the different genotypes (Figure 5A). Interestingly, we observed a 28% increase in total Na<sub>v</sub>1.2 protein levels in SCN2A<sup>V1282F/V1282F</sup> neurons compared to SCN2A<sup>WT/WT</sup> neurons (Figure 5B). Notably, the SCN2A<sup>WT/V1282F</sup> neurons had a level of protein in between the wildtype and homozygous variant neurons. No change in plasma membrane Na<sub>v</sub>1.2 levels was observed (Figure 5C). Together these data demonstrate that the V1282F variant does not inhibit SCN2A expression or SCN2A localization but does slightly increase SCN2A protein levels.

### SCN3A and SCN8A sodium channel gene expression

In addition to Na<sub>v</sub>1.2, other members of the voltage-gated sodium channel family, notably Na<sub>v</sub>1.3 (SCN3A) and Na<sub>v</sub>1.6 (SCN8A), are also significantly expressed in these neurons. We next asked if the V1282F variant might alter the expression of SCN3A or SCN8A, which could also result in changes in Na<sup>+</sup> current density *via* compensatory mechanisms. To address this question, we performed qRT-PCR to quantify the mRNA transcript levels. We identified a 20% increase in SCN3A levels in SCN2A<sup>V1282F/V1282F</sup> neurons, but no change in SCN2A<sup>WT/V1282F</sup> neurons when compared to the SCN2A<sup>WT/WT</sup> neurons. On the other hand, SCN8A levels were not significantly different for the three genotypes (Figure 5A).

## Discussion

Na<sub>v</sub>1.2 variants associated with IEE and BIFS are thought to result in a gain-of-function, whereas those implicated in ASD and ID are thought to result in a loss-of-function. Several Na<sub>v</sub>1.2 variants have also been identified as linked to schizophrenia. However, none of

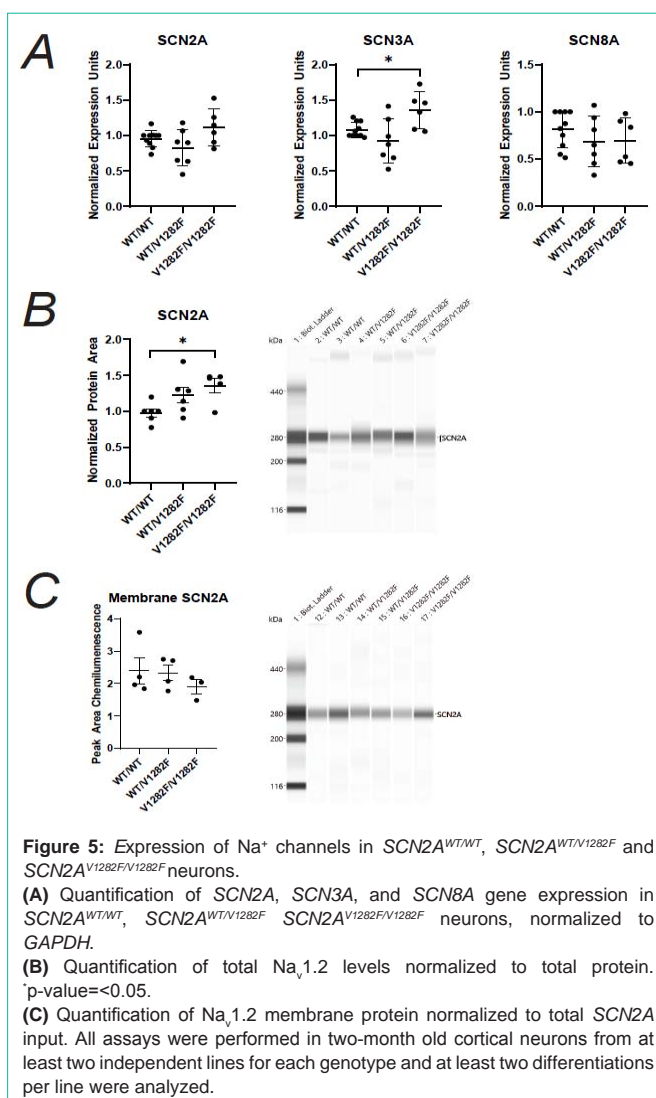


**Figure 5:** Expression of Na<sup>+</sup> channels in SCN2A<sup>WT/WT</sup>, SCN2A<sup>WT/V1282F</sup> and SCN2A<sup>V1282F/V1282F</sup> neurons.

(A) Quantification of SCN2A, SCN3A, and SCN8A gene expression in SCN2A<sup>WT/WT</sup>, SCN2A<sup>WT/V1282F</sup> SCN2A<sup>V1282F/V1282F</sup> neurons, normalized to GAPDH.

(B) Quantification of total Na<sub>v</sub>1.2 levels normalized to total protein. \* $p$ -value =  $< 0.05$ .

(C) Quantification of Na<sub>v</sub>1.2 membrane protein normalized to total SCN2A input. All assays were performed in two-month old cortical neurons from at least two independent lines for each genotype and at least two differentiations per line were analyzed.

them have been functionally investigated. In this report, we studied the effect of the schizophrenia associated SCN2A variant, V1282F, in a native neuronal environment. We engineered the mutation in isogenic hiPSC-derived cortical neurons and assessed Na<sup>+</sup> channel activity as well as other functional and biochemical endpoints and consequences. To our knowledge, this is the first SCN2A variant functionally modeled in hiPSC-derived neurons.

We found that hiPSC-derived cortical neurons containing the V1282F missense mutation in SCN2A have decreased Na<sup>+</sup> current density. Consistent with this, V1282F mutant channel expressed in HEK293 cells produce smaller macroscopic currents than WT channels. As such, our results indicate that V1282F results in loss-of-function phenotypes both in hiPSC-derived neurons and in a heterologous system. Two ASD missense mutations (D82G and T1429M) assessed in HEK293 cells have also been found to have decreased peak currents, supporting the hypothesis that SCN2A schizophrenia variants functionally align with ASD variants over IEE and BIFS variants [12]. The observed increase in SCN3A gene expression in hiPSC-derived neurons may suggest a compensatory mechanism for a decrease in SCN2A function. While we saw a

significant increase in *SCN2A* protein in these neurons, we did not observe a significant difference in *SCN2A* mRNA. This increase in protein could be rationalized by the slight but not significant increase in *SCN2A* mRNA and/or the possibility that the *SCN2A* V1282F protein is more stable. Potentially, the increase in *SCN2A* protein could also be due to a feedback mechanism to compensate for the decrease in Na<sup>+</sup> current, which suggest the neurons are trying to increase channel number to compensate for the functionally impaired protein.

Additionally, our interest lies in how a 25% decrease in current density may affect overall network activity. With the development of new high-density multi-electrode arrays, it is now possible to address this question in future studies. Deneault et al. engineered a *SCN2A* knockout in iPSC-derived neurons and found that *SCN2A*<sup>-/-</sup> neurons had decreased sEPSC frequency but no change in amplitude [20]. Moreover, they used multi-electrode arrays to analyze network activity and found *SCN2A*<sup>-/-</sup> neurons had a decreased mean firing rate and decreased burst frequency [20]. These findings suggest that *SCN2A*<sup>V1282F/V1282F</sup> neurons may also have altered network activity.

While mutations in *SCN2A* do have various effects on Na<sup>+</sup> channel function, as previously shown by others and here by us, how these changes in Na<sup>+</sup> channel activity lead to a pathological mechanism of disease is not well understood. Neuronal electrical activity is required for proper development of the nervous system, specifically in neurite outgrowth, dendritic growth, axon pathfinding and synapse formation [21,22]. Moreover, expression of voltage-gated sodium channels is tightly coordinated during development. As *SCN2A* knockout mice are perinatal lethal, the contribution of *SCN2A* is vital [14]. *SCN2A* is expressed along the length of the axon in early development before it is eventually replaced by *SCN8A*. At this point, *SCN2A* becomes localized to the axon initial segment and nodes of Ranvier [23-25]. A decrease in the effective function of *SCN2A* during these early phases of neurodevelopment could have a lasting impact, for example, later in adolescence and early adulthood when the clinical symptoms of schizophrenia manifest.

The hiPSC-derived cortical neuron cultures used for our studies represent early embryonic cortical development [26]. We propose that we may be modeling the early developmental stages of disease with this *in vitro* culture system, thus the significant difference in activity of the channel in this system likely translates to the early *in vivo* situation. Since our neuronal cultures are more fetal-like than adult, this could be why we did not observe decreased synapse density in our *SCN2A*<sup>V1282F/V1282F</sup> neurons. However, other hiPSC disease modeling studies have reported decreased synapse density [27,28], so another possibility is simply that the V1282F variant does not result in reductions in synapse density. When *SCN2A* mutations linked with ASD were computationally modeled in a mature model system, where *SCN8A* protein is elevated and *SCN2A* protein becomes localized to the axon initial segment, only modest phenotypes were observed [12]. These data suggest that those variants played a more active developmental role in the maturation of the brain, which is important for how we design therapeutics to treat disease. Future studies should elucidate whether *SCN2A* could be a potential therapeutic target, and if so, what the timing and mechanism of intervention would consist of.

The contribution of *SCN2A* variants to neuropsychiatric disease is gaining traction and our data here further reveal that a *SCN2A* schizophrenia risk variant may functionally contribute to disease by impairing Na<sub>v</sub>1.2 channel function and subsequent Na<sup>+</sup> current density. This agrees with evidence from a clinical study that found that schizophrenia patients with poorer cognitive performance had lower levels of *SCN2A* expression, suggesting this gene may be implicated more widely in schizophrenia in general [18].

hiPSC disease modeling studies of rare variants associated with schizophrenia are an important step in understanding the underlying mechanism of disease. Moving forward, the knowledge gained from using these approaches will allow us to understand how certain mutations may lead to dysfunction severe enough to cause disease as well as to discover new therapeutics tailored to the specific dysfunction of that gene. Here we have demonstrated that a rare variant in *SCN2A* identified in two unrelated schizophrenia patients causes decreased Na<sup>+</sup> current. Whether this information can be leveraged into a therapeutic strategy for schizophrenia patients harboring the V1282F mutation is a question for future studies.

## References

- Hilker R, Helenius D, Fagerlund B, Skytthe A, Christensen K, Werge TM, et al. Heritability of Schizophrenia and Schizophrenia Spectrum Based on the Nationwide Danish Twin Register. *Biological Psychiatry*. 2018; 83: 492-498.
- Fromer M, Pocklington A, Kavanagh DH, Williams HJ, Dwyer S, Gormley P, et al. *De novo* mutations in schizophrenia implicate synaptic networks. *Nature*. 2014; 506: 179-184.
- Li J, Cai T, Jiang Y, Chen H, He X, Chen C, Li X, et al. Genes with *de novo* mutations are shared by four neuropsychiatric disorders discovered from NPdenovo database. *Mol Psychiatry*. 2016; 21: 290-297.
- Wolff M, Johannesen KM, Hedrich UBS, Masnada S, Rubboli G, Gardella E, et al. Genetic and phenotypic heterogeneity suggest therapeutic implications in *SCN2A*-related disorders. *Brain*. 2017; 140: 1316-1336.
- Sanders SJ, Campbell AJ, Cottrell JR, Moller RS, Wagner FF, Aldridge AL, et al. Progress in Understanding and Treating *SCN2A*-Mediated Disorders. *Trends Neurosci*. 2018; 41: 442-456.
- Liao Y, Deprez L, Maljevic S, Pitsch J, Claes L, Hristova D, et al. Molecular correlates of age-dependent seizures in an inherited neonatal-infantile epilepsy. *Brain*. 2010; 133: 1403-1414.
- Misra SN, Kahlig KM, George AL. Impaired Na<sub>v</sub>1.2 function and reduced cell surface expression in benign familial neonatal-infantile seizures. *Epilepsia*. 2008; 49: 1535-1545.
- Xu R, Thomas EA, Jenkins M, Gazina EV, Chiu C, Heron SE, et al. A childhood epilepsy mutation reveals a role for developmentally regulated splicing of a sodium channel. *Molecular and Cellular Neuroscience*. 2007; 35: 292-301.
- Lauxmann S, Boutry-Kryza N, Rivier C, Mueller S, Hedrich UBS, Maljevic S, et al. An *SCN2A* mutation in a family with infantile seizures from Madagascar reveals an increased subthreshold Na<sup>+</sup> current. *Epilepsia*. 2013; 54: e117-e121.
- Ogiwara I, Ito K, Sawaishi Y, Osaka H, Mazaki E, Inoue I, et al. *De novo* mutations of voltage-gated sodium channel  $\alpha$ 1 gene *SCN2A* in intractable epilepsies. *Neurology*. 2009; 73: 1046-1053.
- Schwarz N, Hahn A, Bast T, Muller S, Loffler H, Maljevic S, et al. Mutations in the sodium channel gene *SCN2A* cause neonatal epilepsy with late-onset episodic ataxia. *Journal of Neurology*. 2016; 263: 334-343.
- Ben-Shalom R, Keeshen CM, Berrios KN, An JY, Sanders SJ, Bender KJ. Opposing Effects on Na<sub>v</sub>1.2 Function Underlie Differences Between *SCN2A* Variants Observed in Individuals With Autism Spectrum Disorder or Infantile Seizures. *Biol Psychiatry*. 2017; 82: 224-232.

13. Begemann A, Acuna MA, Zweier M, Vincent M, Steindl K, Bachmann-Gagescu R, et al. Further corroboration of distinct functional features in *SCN2A* variants causing intellectual disability or epileptic phenotypes. *Molecular Medicine*. 2019; 25: 6.
14. Planells-Cases R, Caprini M, Zhang J, Rockenstein EM, Rivera RR, Murre C, et al. Neuronal death and perinatal lethality in voltage-gated sodium channel alpha (II)-deficient mice. *Biophys J*. 2000; 78: 2878-2891.
15. Tatsukawa T, Raveau M, Ogiwara I, Hattori S, Miyamoto H, Mazaki E, et al. *SCN2A* haploinsufficient mice display a spectrum of phenotypes affecting anxiety, sociability, memory flexibility and amphetamine CX516 rescues their hyperactivity. *Mol Autism*. 2019; 10: 15.
16. Middleton SJ, Kneller EM, Chen S, Ogiwara I, Montal M, Yamakawa K, et al. Altered hippocampal replay is associated with memory impairment in mice heterozygous for the *Scn2a* gene. *Nature Neuroscience*. 2018; 21: 996-1003.
17. Carroll LS, Woolf R, Ibrahim Y, Williams HJ, Dwyer S, Walters J, et al. Mutation screening of *SCN2A* in schizophrenia and identification of a novel loss-of-function mutation. *Psychiatr Genet*. 2016; 26: 60-65.
18. Dickinson D, Straub RE, Trampush JW, Gao Y, Feng N, Xie B, et al. Differential effects of common variants in *SCN2A* on general cognitive ability, brain physiology, and messenger RNA expression in schizophrenia cases and control individuals. *JAMA Psychiatry*. 2014; 71: 647-656.
19. Suddaby JS, Silver J, So J. Understanding the schizophrenia phenotype in the first patient with the full *SCN2A* phenotypic spectrum. *Psychiatric Genetics*. 2019; 29: 91-94.
20. Deneault E, White SH, Rodrigues DC, Ross PJ, Faheem M, Zaslavsky K, et al. Complete Disruption of Autism-Susceptibility Genes by Gene Editing Predominantly Reduces Functional Connectivity of Isogenic Human Neurons. *Stem Cell Reports*. 2018; 11: 1211-1225.
21. Casagrande VA, Condo GJ. The effect of altered neuronal activity on the development of layers in the lateral geniculate nucleus. *J Neurosci*. 1988; 8: 395-416.
22. Riccio RV, Matthews MA. The postnatal development of the rat primary visual cortex during optic nerve impulse blockade by intraocular tetrodotoxin: a quantitative electron microscopic analysis. *Brain Res*. 1985; 352: 55-68.
23. Garrido JJ, Fernandes F, Giraud P, Mouret I, Pasqualini E, Fache MP, et al. Identification of an axonal determinant in the C-terminus of the sodium channel  $Na_v1.2$ . *The EMBO Journal*. 2001; 20: 5950-5961.
24. Kaplan MR, Cho MH, Ullian EM, Isom LL, Levinson SR, Barres BA. Differential Control of Clustering of the Sodium Channels  $Na_v1.2$  and  $Na_v1.6$  at Developing CNS Nodes of Ranvier. *Neuron*. 2001; 30: 105-119.
25. Kole MHP, Stuart GJ. Signal Processing in the Axon Initial Segment. *Neuron*. 2012; 73: 235-247.
26. Livesey MR, Magnani D, Hardingham GE, Chandran S, Wyllie DJA. Functional properties of *in vitro* excitatory cortical neurons derived from human pluripotent stem cells. *J Physiol*. 2016; 594: 6573-6582.
27. Wen Z, Nguyen HN, Guo Z, Lalli MA, Wang X, Su Y, et al. Synaptic dysregulation in a human iPS cell model of mental disorders. *Nature*. 2014; 515: 414-418.
28. Brennand KJ, Gage FH. Modeling psychiatric disorders through reprogramming. *Dis Model Mech*. 2011; 5: 26-32.